MEAN AND TURBULENT VELOCITY PROFILES FOR SANDGRAIN ROUGH SURFACES

Karen A. Flack, Michael P. Schultz
Department of Mechanical Engineering
United States Naval Academy
Annapolis, Maryland, 21402 USA
flack@usna.edu, mschultz@usna.edu

ABSTRACT

Flat plate turbulent boundary layer measurements have been made on surfaces covered with fine and coarse sandpaper. The measurements were conducted in a closed return water tunnel, over a momentum thickness Reynolds number (Re_θ) range of 3000 to 16000, using a two-component, laser Doppler velocimeter (LDV). The results indicate an increase in the boundary layer thickness (δ), the integral length scales, and the skin-friction coefficient (C_f) for the rough surfaces compared to the smooth wall. The roughness functions (ΔU^+) for the sandgrain surfaces agree within their uncertainty with previous results obtained using towing tank tests and similarity law analysis. For sandpaper, it appears that a single roughness length scale (k = 0.75 R_t) is sufficient to characterize the physical surface. The present results indicate that the mean profiles for both the smooth and rough surfaces collapse well in velocity defect form. The Reynolds stresses also show good collapse outside the roughness sublayer when normalized with the wall shear stress.

INTRODUCTION

While the canonical smooth wall turbulent boundary layer has been extensively investigated through experiments and more recently using direct numerical simulation, turbulent boundary layers developing over roughness have not received as much attention and are much less understood. Many types of rough surfaces occur in engineering applications. Extending results from laboratory type roughness and from one type of surface roughness to another has proven difficult. The mean velocity profile for a number of roughness types has been documented, however the extent the surface roughness affects the mean flow is dependent on the type of roughness element. Few detailed turbulence results exist. The contrary results from these studies also indicate that turbulence is a function of the type of surface roughness. Robust engineering models for flow over rough surfaces rely on the ability to find appropriate scaling parameters for mean and turbulent profiles that are valid for a wide range of roughness element types. In order to accomplish this, detailed measurements need to be obtained for a variety of surfaces. In this investigation, the flow over two sandpaper-type sandgrain rough surfaces will be presented. Sandpaper roughness was selected because it is three-dimensional, which is characteristic of most naturally occurring rough surfaces. Although mean velocity information on sandpaper has been obtained previously, turbulence results are not well documented.

Clauser (1954) argued that the primary effect of surface roughness was to cause a downward shift in the logarithmic region of the mean velocity profile for the boundary layer. For so-called 'k-type' rough walls, the downward shift, ΔU^+, called the roughness function, correlates with k^+, the roughness Reynolds number. Additionally, Townsend (1976) and Perry & Li (1990) state that turbulence is independent of the surface condition outside of the layer of fluid immediately adjacent to the roughness, called the roughness sublayer, at sufficiently high Reynolds number. However, some more recent research indicates that surface roughness alters the velocity defect profile (Krogstad *et al.*, 1992, Acharya *et al.* 1986), leads to a higher degree of isotropy of the Reynolds normal stresses, and changes the Reynolds shear stress profiles in the outer region of the boundary layer (Krogstad *et al.*, 1992, Acharya *et al.* 1986, Antonia & Krogstad, 2001). Another outstanding issue is the ability to characterize the roughness function (ΔU^+) for a generic surface by a physical measurement of the surface roughness (k) alone. Additional detailed tests, which include turbulence data, need to be performed to better understand and predict the effect of surface roughness on turbulence and surface drag.

The effect of uniform sandgrain roughness on the wall shear stress in turbulent pipe flow has been documented dating back to the early work of Nikuradse (1933) and Colebrook and White (1937). These results for uniform sand roughness indicated that there was no measurable increase in the wall shear stress provided that k^+ was less than some critical value. The critical roughness height given by Nikuradse (1933) was k^+ = 3.5. Recently, Bradshaw (2000) has pointed out there is no theoretical justification for the existence of a critical roughness height and states that the increase in wall shear stress should only be zero in the limit as $k^+ \to 0$. It is not clear, therefore, if uniform sand shows an anomalous behavior in the transitionally rough regime or that the necessarily small difference in the wall shear stress when k^+ is small is within the experimental uncertainty.

Bandyopadhyay (1987) studied the mean velocity profiles for turbulent boundary layers on sandpaper surfaces and found roughness functions similar to those of Colebrook and White (1937). Andreopoulos & Bradshaw (1981) present both mean and turbulence profiles for flow over one sandpaper surface in the fully rough regime at a single Reynolds number. Another closely related study is by Ligrani & Moffat (1986) that presents mean and turbulence results for closely packed spheres in the transitionally rough regime. For this type of roughness element, the turbulence quantities collapsed with smooth wall results outside of the roughness sublayer.

While sandgrain surfaces have been previously studied, most experiments have based results on a single rough surface which falls in the fully rough regime. Additionally, detailed turbulence measurements are limited. The goal of the present experimental investigation is to document the mean velocity and Reynolds stress profiles on sandgrain surfaces. One surface falls in the transitionally rough regime while the other is considered fully rough. The surfaces are tested over a range of Reynolds numbers. These are compared with profiles over smooth walls. An attempt to identify a suitable roughness scaling parameter for the roughness function for this particular class of surfaces is made.

EXPERIMENTAL FACILITIES AND METHOD

The present experiments were carried out in the closed circuit water tunnel facility at the United States Naval Academy Hydromechanics Laboratory. The test section is 40 cm by 40 cm in cross-section and is 1.8 m in length, with a tunnel velocity range of 0 – 6.0 m/s. In the present investigation, the freestream velocity was varied between ~1.0 m/s – 3.5 m/s ($Re_x = 1.4\times10^6 - 4.9\times10^6$).

The test specimens were inserted into a flat plate test fixture mounted horizontally in the tunnel. The test fixture is similar to that used by Schultz & Flack (2003). The fixture is 0.40 m in width, 1.68 m in length, and 25 mm thick. The forward most 200 mm of the plate is covered with 36-grit sandpaper to trip the developing boundary layer. The test specimen mounts flush into the test fixture and its forward edge is located immediately downstream of the trip. The removable test specimens are fabricated from 12 mm thick cast acrylic sheet 350 mm in width and 1.32 m in length. The boundary layer profiles presented here were taken 1.35 m downstream of the leading edge of the test fixture. Profiles taken from 0.75 m to the measurement location confirmed that the flow had reached self-similarity. The trailing 150 mm of the flat plate fixture is a movable tail flap. This was set with the trailing edge up at ~5° in the present experiments to prevent separation at the leading edge of the plate. The physical growth of the boundary layer and the inclined tail flap created a slightly favorable pressure gradient at the measurement location. The acceleration parameter (K) varied from 7.4×10^{-8} at the lowest freestream velocity to 2.0×10^{-8} at the highest freestream velocity. The pressure gradient did not vary significantly between the test specimens.

Three test surfaces were tested in the present study. One was a smooth cast acrylic surface. The other two were sandgrain rough surfaces; one covered with 60-grit wet/dry sandpaper and the other with 220-grit wet/dry sandpaper. The surface roughness profiles of the test plates were measured using a Cyber Optics laser diode point range sensor laser profilometer system mounted to a two-axis traverse with a resolution of 5 μm. The resolution of the sensor is 1 μm with a laser spot diameter of 10 μm. Data were taken over a sampling length of 50 mm and were digitized at a sampling interval of 25 μm. Ten linear profiles were taken on each of the test surfaces. No filtering of the profiles was conducted except to remove any linear trend in the trace. The maximum peak to trough roughness height, R_t, for the 60-grit sandpaper was 983 μm, while R_t was 275 μm for the 220-grit sandpaper. The root mean square roughness height, R_q, for the 60-grit sandpaper was 160 μm, while R_q was 38 μm for the 220-grit sandpaper.

Velocity measurements were made using a TSI IFA550 two-component, fiber-optic LDV system. The LDV used a four beam arrangement and was operated in backscatter mode. The probe volume diameter was ~90 μm, and its length was ~1.3 mm. The viscous length (ν/u_τ) varied from a minimum of 5 μm for 60-grit sandpaper at the highest Reynolds number to 24 μm for the smooth wall at the lowest Reynolds number. The diameter of the probe volume, therefore, ranged from 3.8 to 18 viscous lengths in the present study. The LDV probe was mounted on a Velmex three-axis traverse unit. The traverse allowed the position of the probe to be maintained to ± 10 μm in all directions. In order to facilitate two-component, near wall measurements, the probe was tilted downwards at an angle of 4° to the horizontal and was rotated 45° about its axis. Velocity measurements were conducted in coincidence mode with 20,000 random samples per location. Doppler bursts for the two channels were required to fall within a 50 μs coincidence window or the sample was rejected.

In this study, the skin-friction coefficient, C_f, for the smooth surface was found using the Clauser chart method (Clauser, 1954) with log-law constants $\kappa = 0.41$ and $B = 5.0$. For the rough walls, C_f was obtained using a procedure based on the modified Clauser chart method given by Perry & Li (1990). To accomplish this, the wall datum offset was first determined using an iterative procedure. This involved plotting the velocity U/U_e versus $ln\ [(y+\varepsilon)U_e/\nu]$ for points in the log-law region (points between $(y+\varepsilon)^+ = 60$ and $(y+\varepsilon)/\delta = 0.2$) based on an initial guess of u_τ obtained using the total stress method detailed below. The wall datum offset was initially taken to be zero and was increased until the goodness of fit of linear regression through the points was maximized. This was considered the proper wall datum offset. The following formula was then used to determine C_f based on the slope of the regression line (Lewthwaite *et al.*, 1985):

$$C_f = 2\kappa^2\left(\frac{d\left(U/U_e\right)}{d\left(\ln\left[\left(y+\varepsilon\right)U_e/\nu\right]\right)}\right)^2$$

For all three test surfaces, the total stress method was also used to verify C_f. This method assumes a constant stress region equal to the wall shear stress exists in the inner layer of the boundary layer. If the viscous and turbulent stress contributions are added together, an expression for C_f may be calculated as the following evaluated at the total stress plateau in the inner layer:

$$C_f = \frac{2}{U_e^2}\left[\nu\frac{\partial U}{\partial y} - \overline{u'v'}\right]$$

UNCERTAINTY ESTIMATES

Precision uncertainty estimates for the velocity measurements were made through repeatability tests using the procedure given by Moffat (1988). Ten replicate velocity profiles were taken on both a smooth and a rough plate. LDV measurements are also susceptible to a variety of bias errors including angle bias, velocity bias, and velocity gradient bias, as detailed by Edwards (1987). An additional bias error in the v' measurements of ~2% was caused by introduction of the w' component due to inclination of the LDV probe. These bias estimates were combined with the precision uncertainties to calculate the overall uncertainties for the measured quantities. The resulting overall uncertainty in the mean velocity is ±1%. For the turbulence quantities, $\overline{u'^2}$, $\overline{v'^2}$ and, $\overline{u'v'}$ the overall uncertainties are ±2%, ±4%, and ±7%, respectively. The uncertainty in C_f for the smooth walls using the Clauser chart method is ±4%, and the uncertainty in C_f for the rough walls using the modified Clauser chart method was ±7%. The increased uncertainty for the rough walls resulted mainly from the extra two degrees of freedom in fitting the log law (ε and ΔU^+). The uncertainty in C_f using the total stress method is ±8% for both the smooth and rough walls. The uncertainties in δ, δ *, and θ are ±7%, ±4%, and ±5%, respectively.

RESULTS AND DISCUSSION

The experimental conditions for each test case are presented in Table 1. Significant increases in the physical growth of the boundary layer were noted on the sandgrain rough surfaces compared to the smooth wall. The 60-grit sandpaper showed increases of 24%, 70%, and 50%, while the 220-grit sandpaper had increases of 14%, 36%, and 27% in δ, δ^*, and θ, respectively. Figure 1 presents C_f versus Re_θ for the three test surfaces. The smooth wall results of Coles (1962) and DeGraaff & Eaton (2000) are shown for comparison. The sandgrain rough surfaces both exhibited a significant increase in C_f over the entire range of Re_θ. At the highest Reynolds number, C_f was 87% higher than the smooth wall for the 60-grit sandpaper and was 43% higher for the 220-grit sandpaper.

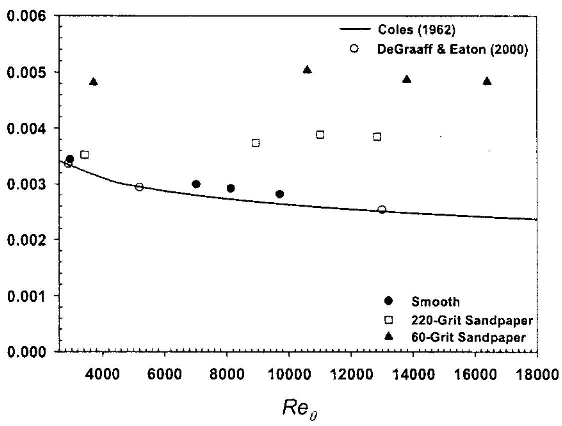

Figure 1. Skin friction coefficient

Table 1. Boundary layer parameters for the test cases.

Specimen	U_e (ms^{-1})	Re_θ	C_f x10^3	δ (mm)	δ* (mm)	θ (mm)	H	ΔU^+
Smooth	0.94	2950	3.44	28	3.8	2.9	1.30	--
	2.60	7020	2.99	26	3.2	2.5	1.27	--
	2.99	8080	2.92	27	3.2	2.5	1.26	--
	3.58	9680	2.82	26	3.2	2.5	1.26	--
60-Grit Sandpaper	0.93	3720	4.82	33	5.1	3.7	1.38	4.5
	2.53	10600	5.04	33	5.5	3.9	1.42	7.4
	3.12	13800	4.87	33	5.9	4.1	1.44	8.0
	3.58	16400	4.84	34	6.1	4.3	1.43	8.3
220-Grit Sandpaper	0.95	3420	3.52	33	4.7	3.5	1.36	1.3
	2.60	8930	3.79	29	4.3	3.2	1.34	3.9
	3.07	11000	3.89	30	4.5	3.3	1.36	4.8
	3.63	12900	3.85	30	4.6	3.4	1.36	5.2

Figure 2 shows the mean velocity profiles in wall variables for the 60-grit and 220-grit sandgrain test surface for the highest Reynolds number. Results for the smooth wall are shown for comparison. The rough surfaces display a linear log region that is shifted by ΔU^+ below the smooth profile, with an increased shift for the rougher surface. Figures 3 and 4 show the mean velocity profiles for the two sandgrain surfaces for a range of Reynolds numbers. The effect of Reynolds number is observed with a trend of increasing ΔU^+ with increasing Re_θ.

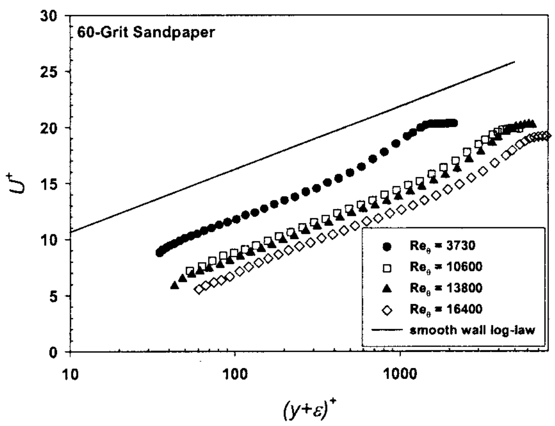

Figure 2. Mean velocity, 60-grit sandpaper

Figure 5 presents the roughness functions (ΔU^+ versus k^+) for all of the sandgrain test surfaces. The Nikuradse-type roughness function (Nikuradse, 1933) for uniform sand given by Schlichting (1979) is shown for comparison, as well as the results from previous sandgrain experiments, Colebrook & White (1937) and Bandyopadhyay (1987). The present sandgrain rough surfaces agree well with a Nikuradse-type roughness function with $k = 0.75\ R_t$. This indicates that for these relatively simple roughness geometries a single roughness height parameter is a sufficient scaling parameter to characterize the physical nature of the surface. Also shown are the results from

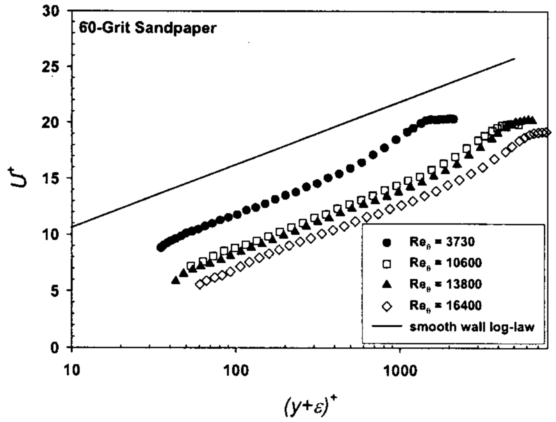

Figure 3. Mean velocity, 60-grit sandpaper

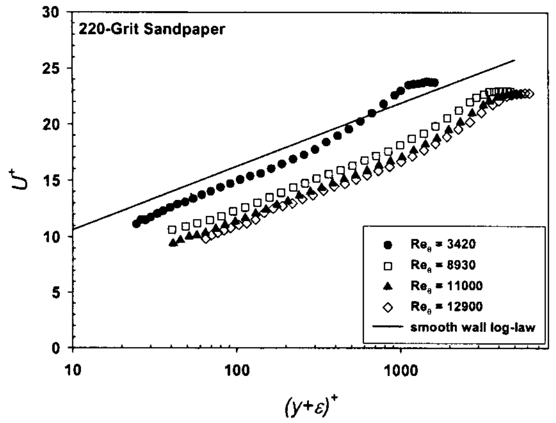

Figure 4. Mean velocity, 220-grit sandpaper

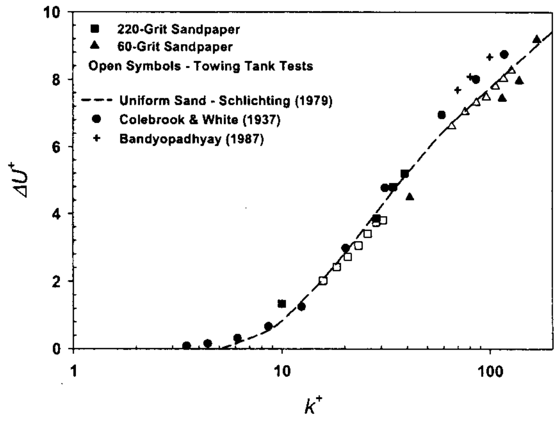

Figure 5. Roughness function, ΔU^+

similar surfaces determined using the overall skin-friction resistance obtained from towing tank measurements and boundary layer similarity law analysis using similar methods as Schultz (2002). Overall, there is fairly good agreement between the data sets and the Nikuradse-type roughness function. This indicates that the roughness functions determined indirectly using overall skin-friction resistance measurements and similarity law analysis can provide results that agree with those determined directly using the mean velocity profile as was argued by Granville (1987).

The mean velocity profiles in defect form for all test surfaces at the highest freestream velocity are presented in Figure 6. The velocity defect profiles exhibit good collapse in the overlap and outer regions of the boundary layer. This supports a universal velocity defect profile for rough and smooth walls, as first proposed by Clauser (1954) and also lends support to the boundary layer similarity hypotheses of Townsend (1976) and Perry & Li (1990) that state that turbulence outside of the roughness sublayer is independent of the surface condition at sufficiently high Reynolds number. A good collapse to a universal defect profile was also observed by Acharya *et al.* (1986) for mesh and machined surface roughness and by Schultz & Flack (2003) for sanded, painted surfaces.

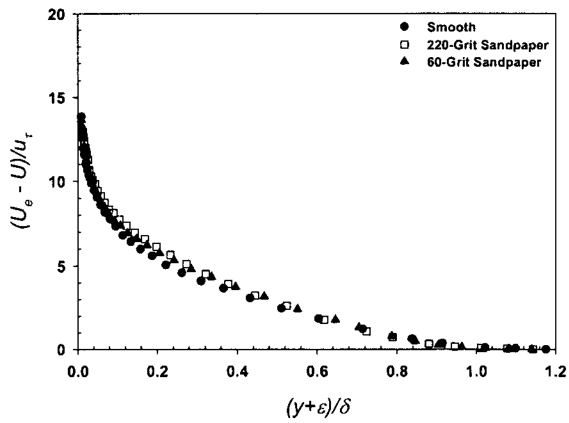

Figure 6. Mean velocity in defect form

The Reynolds normal stress profiles ($\overline{u'^2}/u_\tau^2$ and $\overline{v'^2}/u_\tau^2$) for the sandgrain test surfaces are presented in Figures 7-12. Also shown for comparison are the results of the smooth wall direct numerical simulation (DNS) by Spalart (1988) at Re_θ = 1410. Figures 7 and 8 show $\overline{u'^2}/u_\tau^2$ and $\overline{v'^2}/u_\tau^2$ at the highest freestream velocity for all three surfaces, as well as the smooth and rough (mesh-type) wall experimental results of Perry & Li (1990) at Re_θ = 11097 and 7645, respectively. Good collapse of $\overline{u'^2}/u_\tau^2$ and $\overline{v'^2}/u_\tau^2$ profiles is observed in both the overlap and outer regions of the boundary layer. This is in agreement with the findings of Perry and Li (1990) who also observed no significant difference in the axial and wall-normal Reynolds normal stress profiles for smooth and rough walls outside of the inner region when they were normalized using u_τ^2. Krogstad *et al.* (1992, 1999) and Antonia & Krogstad (2001) also observed no significant difference in the axial Reynolds normal stress profiles, however noted a large increase in $\overline{v'^2}/u_\tau^2$ well into the outer region of the boundary layer for mesh and circular rod roughness.

The Reynolds normal stress profiles for the 220 grit and 60-grit sandgrain surfaces at for a range of Reynolds numbers is shown in Figures 9-12. A good collapse of the The results of the smooth wall DNS by Spalart (1988), the smooth wall experimental results of DeGraaff *et al.* (2000) at Re_θ = 13000, and the rough wall experimental results of Ligrani & Moffat (1986) at Re_θ = 18700 are shown for

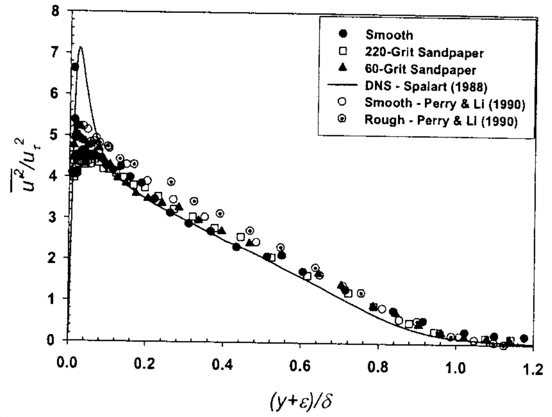

Figure 7. Axial Reynolds normal stress, all surfaces

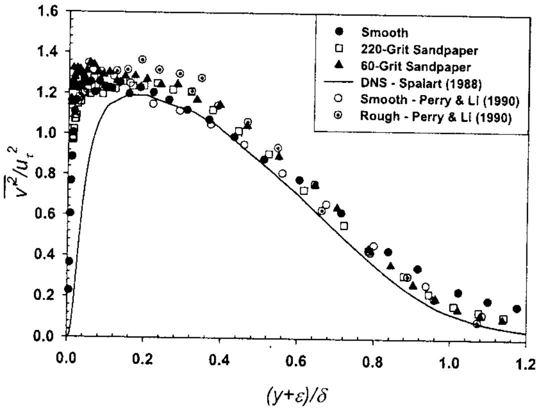

Figure 8. Wall-normal Reynolds normal stress, all surfaces

comparison. Reasonably good collapse of the $-\overline{u'v'}/u_\tau^2$ profiles is observed in both the overlap and outer regions of the boundary layer. On the roughest surface, the 60-grit sandpaper, a local increase in $-\overline{u'v'}/u_\tau^2$ was observed in the inner region of the boundary layer. This increase persisted out to a distance of ~ $4k$ from the wall. Outside of this, the profile collapsed well with the others. There is no discernable effect of Reynolds number, within the uncertainty of the measurements, as indicated on Figures 14 and 15. A reasonable collapse is observed for the entire Reynolds number range.

CONCLUSION

In conclusion, comparisons of turbulent boundary layers developing over sandgrain and smooth surfaces have been made. An increase in the physical growth of the boundary layer as well as an increase in C_f was measured for the sandgrain surfaces. The roughness functions (ΔU^+) for the sandgrain surfaces measured in this study agree within their uncertainty with previous results obtained using towing tank tests and similarity law analysis. For this one simple roughness type, it appears that a single roughness length scale (k = 0.75 R_t) is sufficient to characterize the physical surface. Furthermore, the profiles of the normalized Reynolds stresses ($\overline{u'^2}/u_\tau^2$, $\overline{v'^2}/u_\tau^2$, and $-\overline{u'v'}/u_\tau^2$) for both the smooth and rough surfaces show agreement within experimental uncertainty in the overlap and outer regions of the boundary layer.

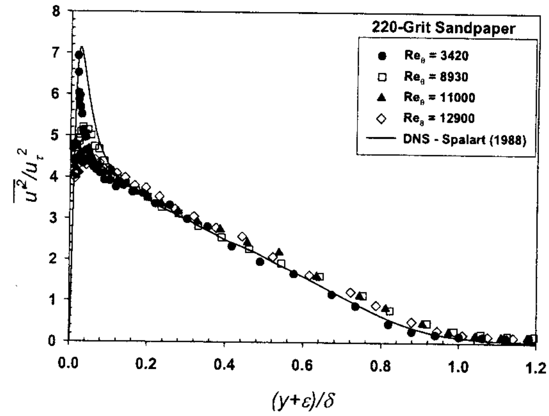

Figure 9. Axial Reynolds normal stress, 220-grit

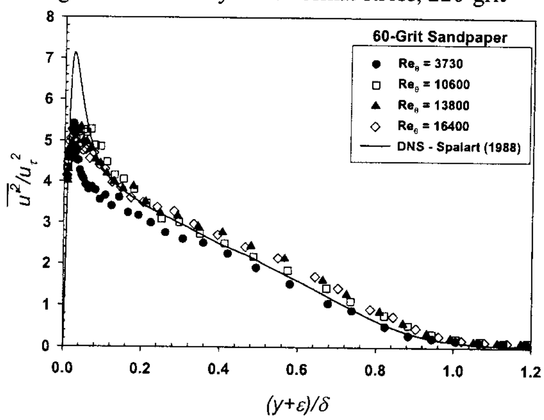

Figure 10. Axial Reynolds normal stress, 60-grit

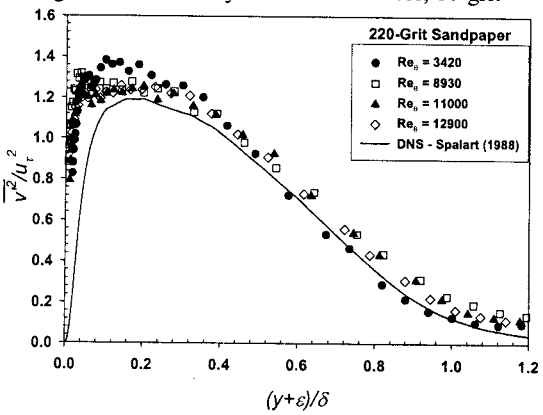

Figure 11. Wall-normal Reynolds normal stress, 220-grit

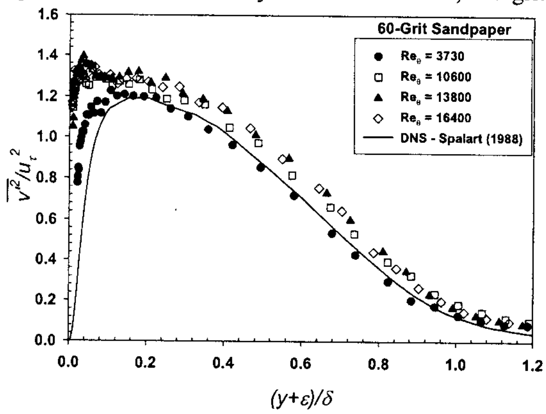

Figure 12. Wall-normal Reynolds normal stress, 60-grit

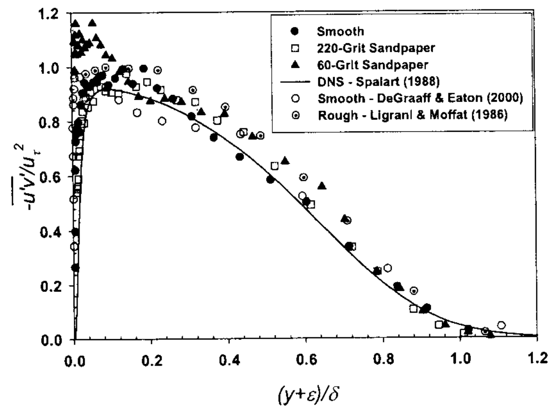

Figure 13. Reynolds shear stress, all surfaces

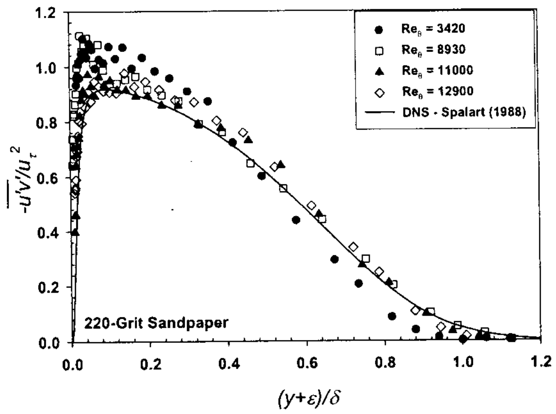

Figure 14. Reynolds shear stress, 220-grit

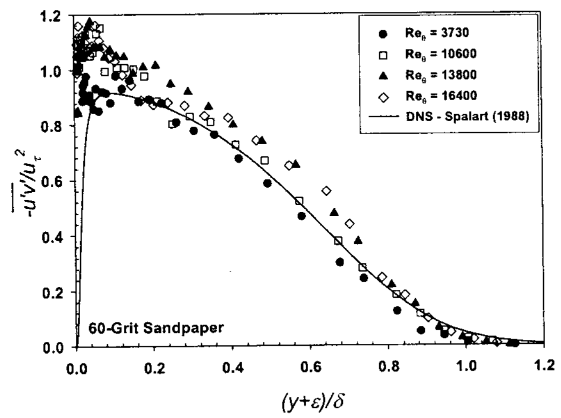

Figure 15. Reynolds shear stress, 60-grit

REFERENCES

Acharya, M., Bornstein, J, and Escudier, M.P., 1986, "Turbulent Boundary Layers on Rough Surfaces," *Experiments in Fluids*, Vol. 4, pp. 33-47.

Andreopoulos J. and Bradshaw, P., 1981, "Measurements of the Turbulence Structure in the Boundary Layer on a Rough Surface," *Boundary-Layer Meteorology*, Vol. 20, pp. 201-213.

Antonia, R.A. and Krogstad, P.-Å., 2001, "Turbulence Structure in Boundary Layers over Different Types of Surface Roughness," *Fluid Dynamics Research*, Vol. 28, pp. 139-157.

Bandyopadhyay, P.R., 1987, "Rough-Wall Turbulent Boundary Layers in the Transition Regime," *Journal of Fluid Mechanics*, Vol. 180, pp. 231-266.

Bradshaw, P., 2000, "A Note on "Critical Roughness Height" and "Transitional Roughness"," *Physics of Fluids*, Vol. 12, pp. 1611-1614.

Clauser, F.H., 1954, "Turbulent Boundary Layers in Adverse Pressure Gradients," *Journal of the Aerospace Sciences*, Vol. 21, pp. 91-108.

Colebrook, C.F. and White, C.M., 1937, "Experiments with Fluid Friction in Roughened Pipes," *Proceedings of the Royal Society*, Vol. 161A, pp. 367-381.

Coles, D., 1962, "The Turbulent Boundary Layer in a Compressible Fluid," The Rand Corp., Rep. R-403-PR.

DeGraaff, D.B. and Eaton, J.K., 2000, "Reynolds-Number Scaling of the Flat-Plate Turbulent Boundary Layer," *Journal of Fluid Mechanics*, Vol. 422, pp. 319-346.

Edwards, R.V., 1987, "Report of the Special Panel on Statistical Particle Bias Problems in Laser Anemometry," *Journal of Fluids Engineering*, Vol. 109, pp. 89-93.

Granville, P.S., 1987, "Three Indirect Methods for the Drag Characterization of Arbitrarily Rough Surfaces on Flat Plates," *Journal of Ship Research*, Vol. 31, pp. 70-77.

Krogstad, P.-Å. and Antonia, R.A., 1999, "Surface Roughness Effects in Turbulent Boundary Layers," *Experiments in Fluids*, Vol. 27, pp. 450-460.

Krogstad, P.-Å., Antonia, R.A., and Browne, L.W.B., 1992, "Comparison Between Rough- and Smooth-Wall Turbulent Boundary Layers," *Journal of Fluid Mechanics*, Vol. 245, pp. 599-617.

Lewthwaite, J.C., Molland, A.F., and Thomas, K.W., 1985, "An Investigation into the Variation of Ship Skin Frictional Resistance with Fouling," *Transactions of the Royal Institute of Naval Architects*, Vol. 127, pp. 269-284.

Ligrani, P.M. and Moffat, R.J., 1986, "Structure of Transitionally Rough and Fully Rough Turbulent Boundary Layers," *Journal of Fluid Mechanics* ,Vol. 162, pp. 69-98.

Moffat, R.J., 1988, "Describing the Uncertainties in Experimental Results," *Exp. Them. Fluid Sci.*, Vol. 1, pp. 3-17.

Nikuradse, J., 1933, "Laws of Flow in Rough Pipes," *NACA Technical Memorandum 1292.*

Perry, A.E. and Li, J.D., 1990, "Experimental Support for the Attached-Eddy Hypothesis in Zero-Pressure Gradient Turbulent Boundary Layers," *Journal of Fluid Mechanics*, Vol. 218, pp. 405-438.

Schlichting, H., 1979, Boundary-Layer Theory, 7th Edition, McGraw-Hill, New York.

Schultz, M.P., 2002, "The Relationship between Frictional Resistance and Roughness for Surfaces Smoothed by Sanding," *J. Fluids Engr.*, Vol. 124, pp. 492-499.

Schultz, M.P. and Flack, K.A., 2003, "Turbulent Boundary Layers over Surfaces Smoothed by Sanding" to appear in *Journal of Fluids Engineering.*

Spalart, P.R., 1988, "Direct Simulation of a Turbulent Boundary Layer up to Re_θ = 1410," *Journal of Fluid Mechanics*, Vol. 187, pp. 61-98.

Townsend, A.A., 1976, The Structure of Turbulent Shear Flow, Cambridge University Press, Cambridge, UK.